Lattice study of rotating QCD properties

Artem Roenko[1],

in collaboration with

V. V. Braguta, M. N. Chernodub, Ya. A. Gershtein, I. E. Kudrov, D. A. Sychev

[1]Joint Institute for Nuclear Research (JINR), Dubna
roenko@theor.jinr.ru

India-JINR Workshop on Particle, Nuclear, Neutrino Physics and Astrophysics,
Bhubaneswar, NISER, 10-12 November 2025

Introduction

- In non-cetral heavy ion collisions, the droplets of QGP with angular momentum are crated.
- The rotation occurs with relativistic velocities, at the same time $\Omega \ll \Lambda_{QCD}$

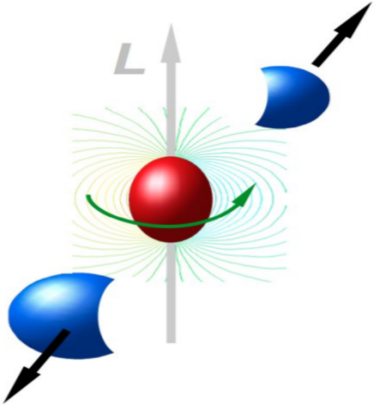

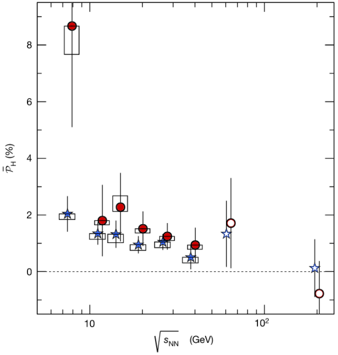

[L. Adamczyk et al. (STAR), Nature **548**, 62–65 (2017), arXiv:1701.06657 [nucl-ex]]

$\omega = 10$ MeV ~ 0.05 fm^{-1} $\quad v \sim c$ at $r \sim 20$ fm

$\langle\omega\rangle \sim 7$ MeV $\quad (\sqrt{s_{NN}}$-averaged$)$

Introduction

- In non-cetral heavy ion collisions, the droplets of QGP with angular momentum are crated.
- The rotation occurs with relativistic velocities, at the same time $\Omega \ll \Lambda_{QCD}$

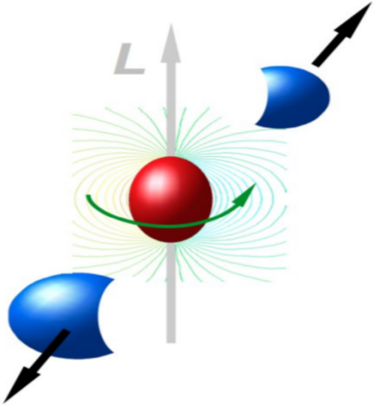

$\omega = 10$ MeV ~ 0.05 fm^{-1} $\quad v \sim c$ at $r \sim 20$ fm

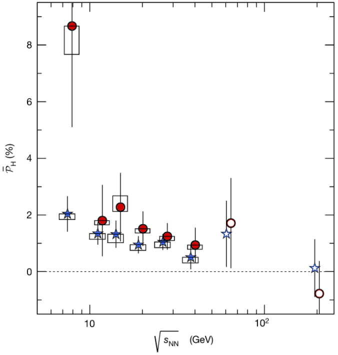

[L. Adamczyk et al. (STAR), Nature **548**, 62–65 (2017), arXiv:1701.06657 [nucl-ex]]

$\langle\omega\rangle \sim 7$ MeV $\left(\sqrt{s_{NN}}\text{-averaged}\right)$

- How does the rotation affect QCD properties?

Formulation of rotating QCD on the lattice

- A. Yamamoto and Y. Hirono, Phys. Rev. Lett. **111**, 081601 (2013), arXiv:1303.6292 [hep-lat]

Bulk-averaged critical temperature in rotating gluodynamics:

- V. Braguta et al., JETP Lett. **112**, 6–12 (2020)
- V. Braguta et al., Phys. Rev. D **103**, 094515 (2021), arXiv:2102.05084 [hep-lat]

Bulk-averaged critical temperature in rotating QCD:

- V. Braguta et al., PoS **LATTICE2022**, 190 (2023), arXiv:2212.03224 [hep-lat]
- J.-C. Yang and X.-G. Huang, (2023), arXiv:2307.05755 [hep-lat]

Thermodynamical properties and moment of inertia of rotating gluon plasma:

- V. V. Braguta et al., Phys. Lett. B **852**, 138604 (2024), arXiv:2303.03147 [hep-lat]
- V. V. Braguta et al., JETP Lett. **117**, 639–644 (2023)
- V. V. Braguta et al., Phys. Rev. D **110**, 014511 (2024), arXiv:2310.16036 [hep-ph]

Mixed inhomogeneous phase in rotating gluon plasma:

- V. V. Braguta, M. N. Chernodub, and A. A. Roenko, Phys. Lett. B **855**, 138783 (2024), arXiv:2312.13994 [hep-lat]
- V. V. Braguta et al., JHEP **09**, 079 (2025), arXiv:2411.15085 [hep-lat]

Rotating QCD in Minkowksi space

It is convenient to describe the system in the co-rotating reference frame, $x^\mu = (t, x, y, z)$,

$$\varphi = [\varphi_{\text{lab}} - \Omega t]_{2\pi}\,, \quad t = t_{\text{lab}}, \quad z = z_{\text{lab}}, \quad r = r_{\text{lab}}, \tag{1}$$

with the metric

$$g_{\mu\nu} = \frac{\partial x^\alpha_{\text{lab}}}{\partial x^\mu}\frac{\partial x^\beta_{\text{lab}}}{\partial x^\nu}\gamma_{\alpha\beta} = \begin{pmatrix} 1 - r^2\Omega^2 & y\Omega & -x\Omega & 0 \\ y\Omega & -1 & 0 & 0 \\ -x\Omega & 0 & -1 & 0 \\ 0 & 0 & 0 & -1 \end{pmatrix}. \tag{2}$$

The Dirac Lagrangian in curved space is given by

$$\mathcal{L}_\psi = \bar{\psi}\left(i\gamma^\mu\left(D_\mu + \Gamma_\mu\right) - m\right)\psi = \mathcal{L}_\psi^{(0)} + \mathcal{L}_\psi^{(1)}\,, \tag{3}$$

and the Lagrangian of Yang-Mills theory in the Minkowski curved spacetime is

$$\mathcal{L}_G = -\frac{1}{4g_{YM}^2} g^{\mu\nu} g^{\alpha\beta} F^a_{\mu\alpha} F^a_{\nu\beta} = \mathcal{L}_G^{(0)} + \mathcal{L}_G^{(1)} + \mathcal{L}_G^{(2)}\,, \tag{4}$$

where $\mathcal{L}^{(n)} \propto \Omega^n$, and $\Omega = \partial_t \varphi_{\text{lab}}$.

Rotating QCD in Minkowksi space

It is convenient to describe the system in the co-rotating reference frame, $x^\mu = (t, x, y, z)$,

$$\varphi = [\varphi_{\rm lab} - \Omega t]_{2\pi}\,, \quad t = t_{\rm lab}, \quad z = z_{\rm lab}, \quad r = r_{\rm lab}, \tag{1}$$

with the metric

$$g_{\mu\nu} = \frac{\partial x^\alpha_{\rm lab}}{\partial x^\mu}\frac{\partial x^\beta_{\rm lab}}{\partial x^\nu}\gamma_{\alpha\beta} = \begin{pmatrix} 1 - r^2\Omega^2 & y\Omega & -x\Omega & 0 \\ y\Omega & -1 & 0 & 0 \\ -x\Omega & 0 & -1 & 0 \\ 0 & 0 & 0 & -1 \end{pmatrix}. \tag{2}$$

The Dirac Lagrangian in curved space is given by

$$\mathcal{L}_\psi = \bar\psi\left(i\gamma^\mu(D_\mu + \Gamma_\mu) - m\right)\psi = \mathcal{L}^{(0)}_\psi + \mathcal{L}^{(1)}_\psi\,, \tag{3}$$

and the Lagrangian of Yang-Mills theory in the Minkowski curved spacetime is

$$\mathcal{L}_G = -\frac{1}{4g^2_{YM}} g^{\mu\nu}g^{\alpha\beta}F^a_{\mu\alpha}F^a_{\nu\beta} = \mathcal{L}^{(0)}_G + \mathcal{L}^{(1)}_G + \mathcal{L}^{(2)}_G\,, \tag{4}$$

where $\mathcal{L}^{(n)} \propto \Omega^n$, and $\Omega = \partial_t\varphi_{\rm lab}$.

The causality restriction: $\boxed{\Omega r < 1}$.

Lattice simulation is a powerful method for studying strong-interacting systems:

- Based on the *path-integral* representation of the partition function:

$$\langle \mathcal{O} \rangle = \frac{1}{\mathcal{Z}} \int \mathcal{D}[A]\mathcal{D}[\psi,\bar{\psi}]\, e^{-S_E(\psi,\bar{\psi},A)}\, \mathcal{O}(\psi,\bar{\psi},A)\,, \qquad \mathcal{Z} = \int \mathcal{D}[A]\mathcal{D}[\psi,\bar{\psi}]\, e^{-S_E(\psi,\bar{\psi},A)}$$

- The spacetime is discretized on the hypercubic Euclidean lattice with finite spacing a.

- In continuum, the discretized action $S_E^{(\mathrm{lat})}$ exactly reproduces S_E.

- The integrals are computed using Monte-Carlo algorithms,

$$\langle \mathcal{O} \rangle = \frac{1}{N_{conf}} \sum_i O(\{U_i\})\,, \quad \text{with} \quad p(\{U_i\}) \sim e^{-S[\{U\}]}\,. \tag{5}$$

- The continuum limit $a \to 0$ should be taken.

- Statistical and systematic uncertainties are under control. HPC is used. [See Talk by V. Braguta]

Rotating QCD in Euclidean space

The rotating system at thermal equilibrium is studied on the lattice. The partition function is

$$\mathcal{Z} = \mathrm{Tr}\left[e^{-\hat{H}/T_0}\right] = \mathrm{Tr}\left[e^{-(\hat{H}_0-\hat{J}\Omega)/T_0}\right] = \int \mathcal{D}[U]\,\mathcal{D}[\psi,\bar{\psi}]\; e^{-S_G[U,\Omega]-S_F[U,\psi,\bar{\psi},\Omega]}\,, \tag{6}$$

where the Euclidean action, $S_G + S_F$, is formulated in curved space $(t \to -i\tau)$, $x^\mu = (x, y, z, \tau)$,

$$g^E_{\mu\nu} = \begin{pmatrix} 1 & 0 & 0 & -y\Omega_I \\ 0 & 1 & 0 & x\Omega_I \\ 0 & 0 & 1 & 0 \\ -y\Omega_I & x\Omega_I & 0 & 1 + r^2\Omega_I^2 \end{pmatrix}, \tag{7}$$

and the angular velocity is imaginary, $\Omega_I = \partial_\tau \varphi_{\mathrm{lab}} = -i\partial_t \varphi_{\mathrm{lab}} = -i\Omega$, to avoid the sign problem.

There is no causality restriction in Euclidean space.

Rotating QCD in Euclidean space

The rotating system at thermal equilibrium is studied on the lattice. The partition function is

$$\mathcal{Z} = \mathrm{Tr}\left[e^{-\hat{H}/T_0}\right] = \mathrm{Tr}\left[e^{-(\hat{H}_0-\hat{J}\Omega)/T_0}\right] = \int \mathcal{D}[U]\,\mathcal{D}[\psi,\bar{\psi}]\; e^{-S_G[U,\Omega]-S_F[U,\psi,\bar{\psi},\Omega]}\,, \tag{6}$$

where the Euclidean action, $S_G + S_F$, is formulated in curved space ($t \to -i\tau$), $x^\mu = (x, y, z, \tau)$,

$$g^E_{\mu\nu} = \begin{pmatrix} 1 & 0 & 0 & -y\Omega_I \\ 0 & 1 & 0 & x\Omega_I \\ 0 & 0 & 1 & 0 \\ -y\Omega_I & x\Omega_I & 0 & 1 + r^2\Omega_I^2 \end{pmatrix}, \tag{7}$$

and the angular velocity is imaginary, $\Omega_I = \partial_\tau \varphi_{\mathrm{lab}} = -i\partial_t \varphi_{\mathrm{lab}} = -i\Omega$, to avoid the sign problem.

There is no causality restriction in Euclidean space.

- The inverse temperature $1/T_0$ sets the system length in τ-direction.
- Tolman–Ehrenfest (TE) law: the local temperature *depends on the coordinates*

$$T(r)\sqrt{g_{00}} = T(r)\sqrt{1 - r^2\Omega^2} = T(r)\sqrt{1 + r^2\Omega_I^2} = T_0\,.$$

- We will use the notation $T \equiv T_0 = T(r = 0)$.

The quark action is a linear function in angular velocity:

$$S_\psi = \int d^4x\,\sqrt{g_E}\,\bar\psi\left(\gamma^\mu(\partial_\mu + \Gamma_\mu) + m\right)\psi = S_0^\psi + S_1^\psi\Omega_I =$$

$$= \int d^4x\,\bar\psi\left(\left(\gamma^1 + y\Omega_I\gamma^4\right)D_x + \left(\gamma^2 - x\Omega_I\gamma^4\right)D_y + \gamma^3 D_z + \gamma^4\left(D_\tau + i\Omega_I\frac{\sigma^{12}}{2}\right) + m\right)\psi\,, \qquad (8)$$

The gluon action is a quadratic function in angular velocity:

$$S_G = \frac{1}{4g_{YM}^2}\int d^4x\,\sqrt{g_E}\,g_E^{\mu\nu}\,g_E^{\alpha\beta}F^a_{\mu\alpha}F^a_{\nu\beta} \equiv S_0 + S_1\Omega_I + S_2\frac{\Omega_I^2}{2} =$$

$$= \frac{1}{g_{YM}^2}\int d^4x\left(\frac{1}{4}F^a_{\mu\nu}F^a_{\mu\nu} + \Omega_I\left[-yF^a_{xy}F^a_{y\tau} - yF^a_{xz}F^a_{z\tau} + xF^a_{yx}F^a_{x\tau} + xF^a_{yz}F^a_{z\tau}\right] + \right.$$

$$\left. + \Omega_I^2\left[r^2(F^a_{xy})^2 + y^2(F^a_{xz})^2 + x^2(F^a_{yz})^2 + 2xyF^a_{xz}F^a_{zy}\right]\right) \qquad (9)$$

So, for quarks $\mathcal{L}_\psi^{(1)} = \bar\psi(\boldsymbol{\Omega}\cdot\hat{\boldsymbol{J}})\psi$ (note $\hat{\boldsymbol{J}} = \hat{\boldsymbol{L}} + \hat{\boldsymbol{S}}$), whereas for gluons $\mathcal{L}_G^{(1)} = \boldsymbol{\Omega}\cdot\boldsymbol{J}_G$ and $\mathcal{L}_G^{(2)} \propto B^2$.

▷ sign problem ▷ inhomogeneous action ▷ asymmetry between E^2 and B^2

Causality restriction

- Analytic continuation is allowed only for bounded system with $\Omega r < 1$
- Boundary conditions are important! (they influence the result in all approaches)

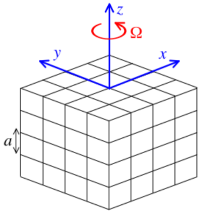

[A. Yamamoto and Y. Hirono, Phys. Rev. Lett. **111**, 081601 (2013), arXiv:1303.6292 [hep-lat]]

- Lattice size: $N_t \times N_z \times N_s^2$ $(N_x = N_y = N_s)$
- "Radius" of the square cylinder: $R = a(N_s - 1)/2$
- Boundary velocity: $v_I^2 = (\Omega_I R)^2 < 1/2$
  (velocity of the corner is $\sqrt{2} v_I$)
- periodic b.c. in directions τ, z.
- different types of b.c. in directions x,y:
  open / periodic / Dirichlet / ...

Let's consider the rotating gluons first.

We use tree-level improved (Symanzik) lattice action for S_0 and chair/plaquette discretization for S_1, S_2.[1]

The temperature is $T = 1/N_t a$. It coincides with the temperature on the rotation axis.

Observables

The Polyakov loop is an order parameter in gluodynamics ($\mathbb{Z}_3$ symmetry),

$$L(\boldsymbol{r}) = \mathrm{Tr}\,\mathcal{P}\exp\left(\oint_0^{1/T} d\tau A_4(\tau, \boldsymbol{r})\right), \tag{10}$$

the lattice form reads as

$$L(x,y) = \frac{1}{N_z}\sum_z \mathrm{Tr}\left[\prod_{\tau=0}^{N_t-1} U_4(\boldsymbol{r},\tau)\right], \qquad L = \frac{1}{N_s^2}\sum_{x,y} L(x,y)\,. \tag{11}$$

In confinement $\langle L\rangle = 0$; in deconfinement $\langle L\rangle \neq 0$. $\langle L\rangle = e^{-F_Q/T}$

The local critical temperature is associated with the peak of the local Polyakov loop susceptibility

$$\chi_L(r) = \langle |L(r)|^2\rangle - \langle |L(r)|\rangle^2\,. \tag{12}$$

[1] V. Braguta et al., Phys. Rev. D **103**, 094515 (2021), arXiv:2102.05084 [hep-lat].

Inhomogeneous phases for imaginary rotation

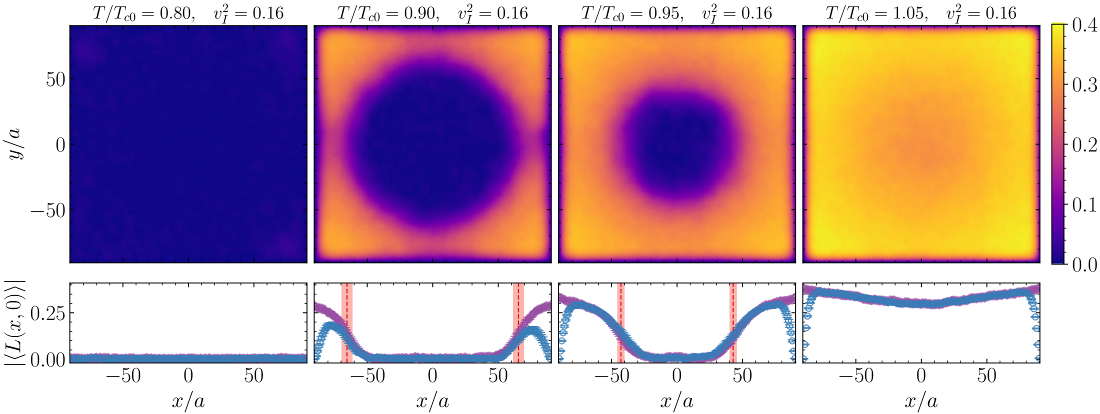

Figure: The distribution of the local Polyakov loop in x, y-plane for the lattice of size $5 \times 30 \times 181^2$ at the fixed imaginary velocity at the boundary $v_I^2 \equiv (\Omega_I R)^2 = 0.16$ and different on-axis temperatures, $T = 1/N_t a$.

- As the (on-axis) temperature increases, the radius of the inner confining region shrinks.
- Boundary is screened; Rotating symmetry is restored.
- Local thermalization takes place; Phase transition occurs as a vortex evolution.

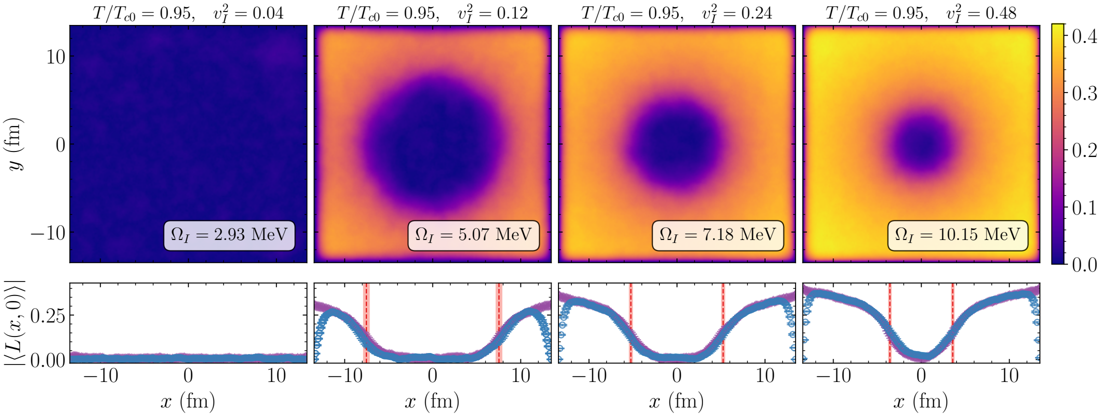

Figure: The distribution of the local Polyakov loop in x, y-plane for the lattice of size $5 \times 30 \times 181^2$ at the fixed temperature $T = 0.95\,T_{c0}$ and different Ω_I; System size $R = 13.5$ fm.

- Mixed inhomogeneous phase takes place at $T \lesssim T_{c0}$. For imaginary rotation, deconfinement appears at the periphery; confinement is in the central regions.
- The confinement region shrinks with the increase in Ω_I;

Local critical temperature

The local critical temperature $T_c(r)$ is the temperature (at the rotation axis) when the phase transition occurs at radius r.

- Lattice parameters: $4 \times 24 \times 145^2$, $5 \times 30 \times 181^2$, $6 \times 36 \times 216^2$, with $v_I^2 = 0.04, \ldots, 0.48$.

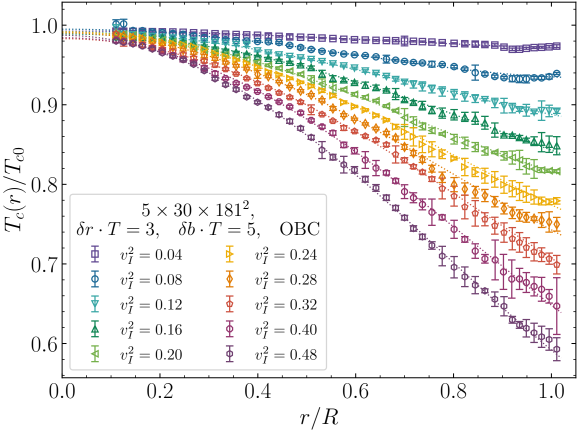

- Results: The local critical temperature decreases with imaginary angular velocity.

$$\frac{T_c(r,\Omega_I)}{T_{c0}} = 1 - \kappa_2(\Omega_I r)^2 - \kappa_4 \left(\frac{r}{R}\right)^2 (\Omega_I r)^2 \quad (13)$$

- The continuum limit result of the quadratic coefficient in the bulk (from quadratic fit) is

$$\kappa_2 = 0.902(33)\,, \quad (14)$$

(next terms are affected by b.c.)

- How analytically continue the inhomogeneous phase?

Decomposition of rotating action for gluons

The action of rotating gluons is inhomogeneous and it is a quadratic function in Ω_I,

$$S_G = S_0 + \lambda_1 S_1 \Omega_I + \lambda_2 S_2 \Omega_I^2 \,, \tag{15}$$

where we introduce switching factors λ_1, λ_2; and operators S_1, S_2 are inhomogeneous.

- No sign problem in a case of $\lambda_1 = 0$. Re2: $\lambda_2 \Omega_I^2 = \Omega_I^2 < 0$ or $\Omega^2 > 0$; Im2: $\lambda_2 \Omega_I^2 = \Omega_I^2 > 0$

Decomposition of rotating action for gluons

The action of rotating gluons is inhomogeneous and it is a quadratic function in Ω_I,

$$S_G = S_0 + \lambda_1 S_1 \Omega_I + \lambda_2 S_2 \Omega_I^2 \,, \tag{15}$$

where we introduce switching factors λ_1, λ_2; and operators S_1, S_2 are inhomogeneous.

- No sign problem in a case of $\lambda_1 = 0$. Re2: $\lambda_2 \Omega_I^2 = \Omega_I^2 < 0$ or $\Omega^2 > 0$; Im2: $\lambda_2 \Omega_I^2 = \Omega_I^2 > 0$

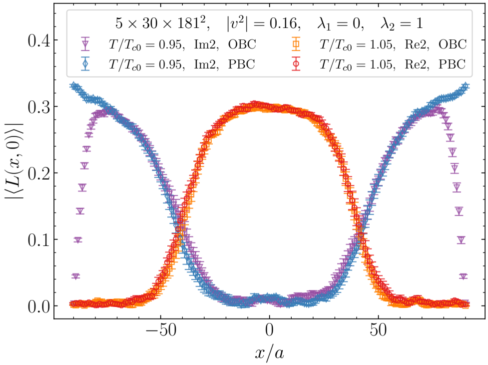

- Re2: $T = T_{c0} + \Delta T$ vs Im2: $T = T_{c0} - \Delta T$

$$\frac{T_c(r,\Omega)}{T_{c0}} = 1 + \kappa(\Omega r)^2 \quad \text{vs} \quad \frac{T_c(r,\Omega_I)}{T_{c0}} = 1 - \kappa(\Omega_I r)^2$$

Decomposition of rotating action for gluons

The action of rotating gluons is inhomogeneous and it is a quadratic function in Ω_I,

$$S_G = S_0 + \lambda_1 S_1 \Omega_I + \lambda_2 S_2 \Omega_I^2 \,, \tag{15}$$

where we introduce switching factors λ_1, λ_2; and operators S_1, S_2 are inhomogeneous.

- No sign problem in a case of $\lambda_1 = 0$. Re2: $\lambda_2 \Omega_I^2 = \Omega_I^2 < 0$ or $\Omega^2 > 0$; Im2: $\lambda_2 \Omega_I^2 = \Omega_I^2 > 0$

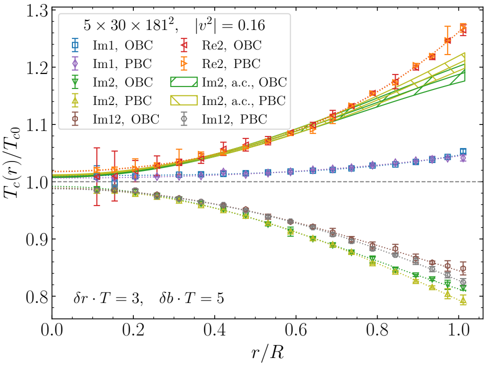

- Re2: $T = T_{c0} + \Delta T$ vs Im2: $T = T_{c0} - \Delta T$

  $$\frac{T_c(r,\Omega)}{T_{c0}} = 1 + \kappa(\Omega r)^2 \quad \text{vs} \quad \frac{T_c(r,\Omega_I)}{T_{c0}} = 1 - \kappa(\Omega_I r)^2$$

- The Re2-regime is in agreement with a.c. of the Im2-results in a bulk.
- S_1 and S_2 have opposite influence on T_c.
- Effect of E^2/B^2-asymmetry (S_2) dominates.

Local approximation for inhomogeneous action

The homogeneous local action (at $x = r_0$, $y = 0$) is

$$S_G = \frac{1}{2g_0^2} \int d^4x \left[F^a_{x\tau} F^a_{x\tau} + F^a_{y\tau} F^a_{y\tau} + F^a_{z\tau} F^a_{z\tau} + F^a_{xz} F^a_{xz} + \right.$$
$$\left. + \left(1 + u_I^2\right) F^a_{yz} F^a_{yz} + \left(1 + u_I^2\right) F^a_{xy} F^a_{xy} - 2u_I \left(F^a_{yx} F^a_{x\tau} + F^a_{yz} F^a_{z\tau} \right) \right], \quad (16)$$

where $u_I = \Omega_I r_0$ is a local velocity. Local system is simulated as usual on small lattices with $N_s = N_z$.

The homogeneous local action (at $x = r_0$, $y = 0$) is

$$S_G = \frac{1}{2g_0^2} \int d^4x \left[F^a_{x\tau}F^a_{x\tau} + F^a_{y\tau}F^a_{y\tau} + F^a_{z\tau}F^a_{z\tau} + F^a_{xz}F^a_{xz} + \right.$$
$$\left. + \left(1 + u_I^2\right) F^a_{yz}F^a_{yz} + \left(1 + u_I^2\right) F^a_{xy}F^a_{xy} - 2u_I \left(F^a_{yx}F^a_{x\tau} + F^a_{yz}F^a_{z\tau} \right) \right], \quad (16)$$

where $u_I = \Omega_I r_0$ is a local velocity. Local system is simulated as usual on small lattices with $N_s = N_z$.

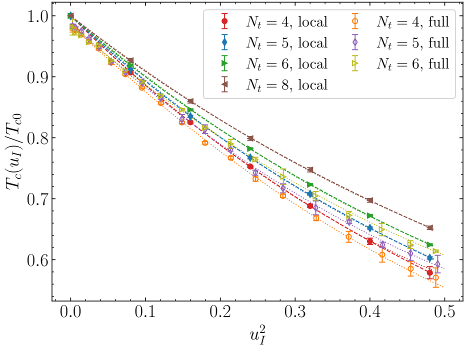

- $T_c(u)$ from two methods are in agreement.
- Data are fitted by two different functions:

$$\frac{T_c(u_I)}{T_{c0}} = 1 + k_2 u^2 + k_4 u^4 \,, \quad (17)$$

$$\frac{T_c(u)}{T_{c0}} = \frac{1 + c_2 u^2}{1 - b_2 u^2} \,. \quad (18)$$

The homogeneous local action (at $x = r_0$, $y = 0$) is

$$S_G = \frac{1}{2g_0^2} \int d^4x \left[F^a_{x\tau}F^a_{x\tau} + F^a_{y\tau}F^a_{y\tau} + F^a_{z\tau}F^a_{z\tau} + F^a_{xz}F^a_{xz} + \right.$$
$$\left. + \left(1 + u_I^2\right) F^a_{yz}F^a_{yz} + \left(1 + u_I^2\right) F^a_{xy}F^a_{xy} - 2u_I \left(F^a_{yx}F^a_{x\tau} + F^a_{yz}F^a_{z\tau}\right) \right], \quad (16)$$

where $u_I = \Omega_I r_0$ is a local velocity. Local system is simulated as usual on small lattices with $N_s = N_z$.

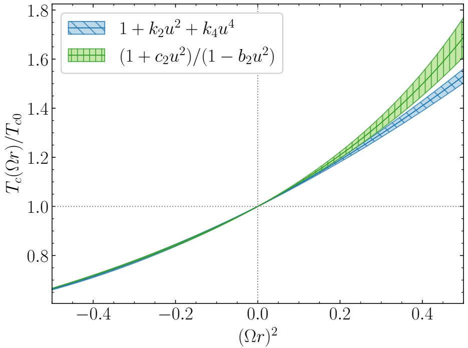

- $T_c(u)$ from two methods are in agreement.
- Data are fitted by two different functions:

$$\frac{T_c(u_I)}{T_{c0}} = 1 + k_2u^2 + k_4u^4\,, \quad (17)$$
$$\frac{T_c(u)}{T_{c0}} = \frac{1 + c_2u^2}{1 - b_2u^2}\,. \quad (18)$$

- In continuum limit the coefficients are

$$k_2 = 0.869(31)\,, \qquad k_4 = 0.388(53)\,. \quad (19)$$
$$c_2 = 0.206(66)\,, \qquad b_2 = 0.694(101)\,. \quad (20)$$

The homogeneous local action (at $x = r_0$, $y = 0$) is

$$S_G = \frac{1}{2g_0^2} \int d^4x \left[F^a_{x\tau}F^a_{x\tau} + F^a_{y\tau}F^a_{y\tau} + F^a_{z\tau}F^a_{z\tau} + F^a_{xz}F^a_{xz} + \right.$$
$$\left. + \left(1 + u_I^2\right) F^a_{yz}F^a_{yz} + \left(1 + u_I^2\right) F^a_{xy}F^a_{xy} - 2u_I \left(F^a_{yx}F^a_{x\tau} + F^a_{yz}F^a_{z\tau} \right) \right], \quad (16)$$

where $u_I = \Omega_I r_0$ is a local velocity. Local system is simulated as usual on small lattices with $N_s = N_z$.

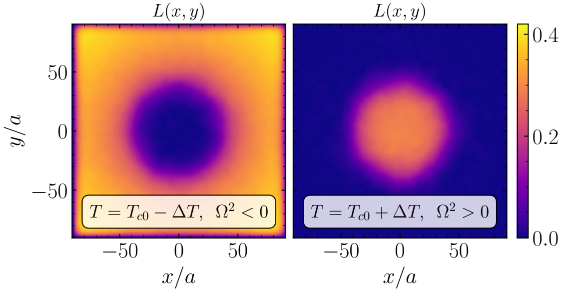

- $T_c(u)$ from two methods are in agreement.
- Data are fitted by two different functions:

$$\frac{T_c(u_I)}{T_{c0}} = 1 + k_2 u^2 + k_4 u^4 \,, \quad (17)$$
$$\frac{T_c(u)}{T_{c0}} = \frac{1 + c_2 u^2}{1 - b_2 u^2} \,. \quad (18)$$

- In continuum limit the coefficients are

$$k_2 = 0.869(31)\,, \qquad k_4 = 0.388(53)\,. \quad (19)$$
$$c_2 = 0.206(66)\,, \qquad b_2 = 0.694(101)\,. \quad (20)$$

Tolman–Ehrenfest effect in rotating (Q)GP

Tolman–Ehrenfest effect: In gravitational field the temperature isn't a constant in space at thermal equilibrium, $T(r)\sqrt{g_{00}} = T_0 = \text{const}$. In the co-rotating reference frame:

$$T(r) = \frac{T_0}{\sqrt{1 - \Omega^2 r^2}} = \frac{T_0}{\sqrt{1 + \Omega_I^2 r^2}} \,. \tag{21}$$

TE law suggests that the rotation effectively heats the periphery. Let's derive $T_c^{TE}(u)$ from an assumption $T(r) = T_{c0}$, it decreases:

$$\frac{T_c^{TE}(u)}{T_{c0}} = \sqrt{1 - u^2} \approx 1 - 0.5u^2 + \dots \,, \tag{22}$$

In the result, TE predicts confinement in the center and deconfinement at the periphery (for *real* rotation).

Tolman–Ehrenfest effect in rotating (Q)GP

Tolman–Ehrenfest effect: In gravitational field the temperature isn't a constant in space at thermal equilibrium, $T(r)\sqrt{g_{00}} = T_0 = \text{const}$. In the co-rotating reference frame:

$$T(r) = \frac{T_0}{\sqrt{1 - \Omega^2 r^2}} = \frac{T_0}{\sqrt{1 + \Omega_I^2 r^2}} \,. \tag{21}$$

TE law suggests that the rotation effectively heats the periphery. Let's derive $T_c^{TE}(u)$ from an assumption $T(r) = T_{c0}$, it decreases:

$$\frac{T_c^{TE}(u)}{T_{c0}} = \sqrt{1 - u^2} \approx 1 - 0.5u^2 + \dots \,, \tag{22}$$

In the result, TE predicts confinement in the center and deconfinement at the periphery (for *real* rotation).

External gravitational field generates asymmetry in the coupling constants of different components of the fields $(F_{\mu\nu})^2$, which influences the dynamics of gluons. This mechanism can not be accounted for by TE.

$$S_G = \int d^4x \left[\beta\left((F^a_{x\tau})^2 + (F^a_{y\tau})^2 + (F^a_{z\tau})^2 + (F^a_{xz})^2\right) + \tilde\beta\left((F^a_{yz})^2 + (F^a_{xy})^2\right)\right], \tag{23}$$

where $\beta = \frac{1}{2} g_{YM}^2$ and $\tilde\beta = \left(1 - (\Omega r_0)^2\right)\beta \equiv \left(1 + (\Omega_I r_0)^2\right)\beta$.

- $\tilde\beta/\beta > 1$ (imaginary rotation) $\Rightarrow$ T_c decreases;
- $\tilde\beta/\beta < 1$ (real rotation) $\Rightarrow$ T_c increases.

Equation of State and Moment of Inertia

The energy of a thermodynamic ensemble in co-rotating reference frame is

$$E = E^{(lab)} - \boldsymbol{J} \cdot \boldsymbol{\Omega}\,, \qquad F = E - TS\,, \qquad dF = -SdT - \boldsymbol{J} \cdot d\boldsymbol{\Omega} + \ldots\,,$$

The moment of inertia is a scalar quantity, $\boldsymbol{J} = I(T,\Omega)\boldsymbol{\Omega}$,

$$I(T,\Omega) = \frac{J(T,\Omega)}{\Omega} = -\frac{1}{\Omega}\left(\frac{\partial F}{\partial \Omega}\right)_T\,,$$

For a classical system with characteristic radius R the moment of inertia is given by

$$I(T,\Omega) = \int_V d^3x\, x_\perp^2 \rho(T, x_\perp, \Omega) \simeq \alpha\, \rho_0(T) V R^2\,,$$

The free energy may be represented as a series in angular velocity (or linear velocity $v_R = \Omega R$)

$$F(T,V,\Omega) = F_0(T,V) - \frac{F_2(T,V)}{2}\Omega^2 + \mathcal{O}(\Omega^4) \equiv F_0(T,V) - \frac{\mathsf{i}_2(T)}{2} V v_R^2 + \mathcal{O}(v_R^4)\,,$$

where $F_2(T,V) = I(T,V,\Omega=0) \equiv \mathsf{i}_2(T) V R^2$, and $\mathsf{i}_2(T)$ is a *specific* moment of inertia.

There are two ways to calculate I: ▷ a.c. of Ω_I-results ▷ derivative $\partial^2 \log Z/\partial \Omega^2$ at $\Omega = 0$

Symanzik gauge action; we calculate $f = F/V$ using standard relations

$$\frac{f(T)}{T^4} = -N_t^4 \int_{\beta_0}^{\beta} d\beta' \Delta s(\beta')\,,$$

where $\Delta s(\beta) = \langle s(\beta)\rangle_{T=0} - \langle s(\beta)\rangle_T \equiv -\langle\!\langle s \rangle\!\rangle$.

- $N_t \times 40 \times 41^2$ lattices with $N_t = 5, 6, 7, 8$;
- $N_t^{(T=0)} = 40$ for $T = 0$ subtraction;
- $v_I^2 \ll 1$, where $v_I = \Omega_I R$, $R = a(N_s - 1)/2$.
- $v_I = \text{const} \quad \Leftrightarrow \quad \Omega_I/T = v_I/RT = \text{const}.$
- $T_c \searrow$ with the imaginary angular velocity.
- Fit by the quadratic function ($f_0 = -p < 0$):

$$f(T, v_I) = f_0(T)\Big(1 - \frac{1}{2}K_2(T)v_I^2\Big)\,.$$

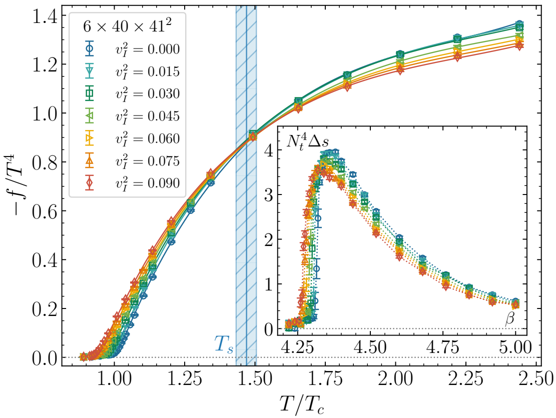

[V. V. Braguta et al., Phys. Lett. B **852**, 138604 (2024), arXiv:2303.03147 [hep-lat]]

- The moment of inertia of gluon plasma

$$I(T)|_{\Omega=0} = -K_2 F_0 R^2\,, \quad K_2 = \mathrm{i}_2/(-f_0)\,,$$

becomes zero at "supervortical" temperature

$$T_s = 1.50(10) T_c.$$

and it is negative for $T < T_s$.

- The result for the system with OBC is

$$T_s = 1.53(15) T_c$$

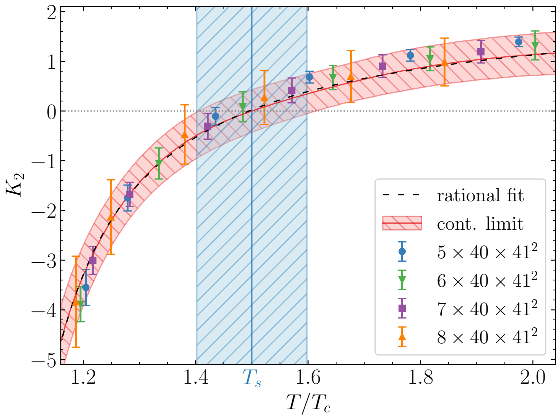

[V. V. Braguta et al., Phys. Lett. B **852**, 138604 (2024), arXiv:2303.03147 [hep-lat]]

Taking the derivative at $\Omega = 0$, we obtain:

$$I = F_2 = T \frac{\partial^2 \log Z}{\partial \Omega^2}\bigg|_{\Omega=0} = T\left(\langle\langle S_1^2 \rangle\rangle_T + \langle\langle S_2 \rangle\rangle_T\right),$$

where $\langle\langle \mathcal{O} \rangle\rangle_T = \langle \mathcal{O} \rangle_T - \langle \mathcal{O} \rangle_{T=0}$.

$$4 f_2/(T^4 L_s^2) \equiv \mathrm{i}_2/T^4\,,$$

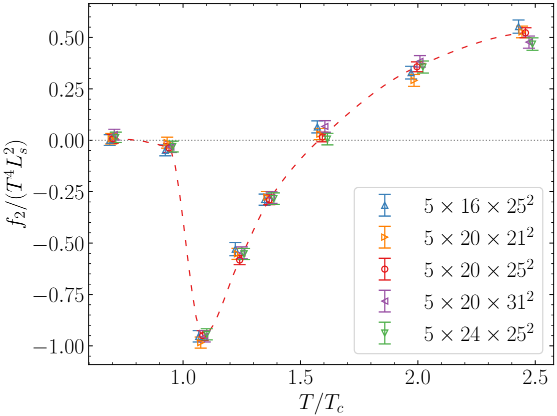

[V. V. Braguta et al., JETP Lett. **117**, 639–644 (2023)]

Taking the derivative at $\Omega = 0$, we obtain:

$$I = F_2 = T \frac{\partial^2 \log Z}{\partial \Omega^2}\bigg|_{\Omega=0} = T\big(\langle\langle S_1^2 \rangle\rangle_T + \langle\langle S_2 \rangle\rangle_T\big)\,,$$

where $\langle\langle \mathcal{O} \rangle\rangle_T = \langle \mathcal{O} \rangle_T - \langle \mathcal{O} \rangle_{T=0}$.

$$4 f_2/(T^4 L_s^2) \equiv \mathrm{i}_2/T^4\,,$$

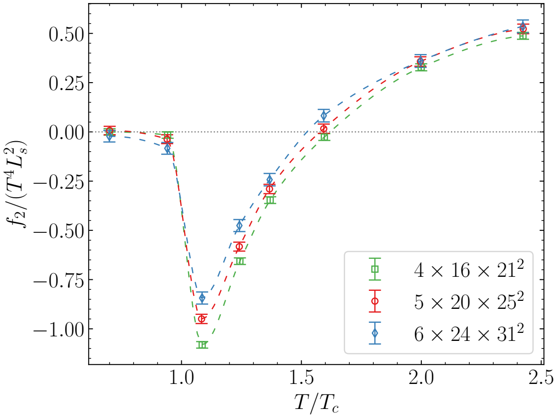

[V. V. Braguta et al., JETP Lett. **117**, 639–644 (2023)]

Results of lattice simulations with zero angular velocity

Taking the derivative at $\Omega = 0$, we obtain:

$$I = F_2 = T \frac{\partial^2 \log Z}{\partial \Omega^2}\bigg|_{\Omega=0} = T\big(\langle\!\langle S_1^2 \rangle\!\rangle_T + \langle\!\langle S_2 \rangle\!\rangle_T\big)\,,$$

where $\langle\!\langle \mathcal{O} \rangle\!\rangle_T = \langle \mathcal{O} \rangle_T - \langle \mathcal{O} \rangle_{T=0}$.

$$4 f_2/(T^4 L_s^2) \equiv \mathsf{i}_2/T^4\,, \qquad K_2 = \mathsf{i}_2/(-f_0)$$

Results of two methods (a.c. from Ω_I and $\partial_\Omega|_{\Omega=0}$) are in agreement.

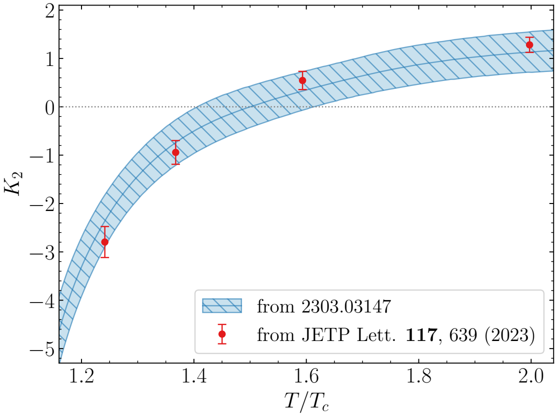

[V. V. Braguta et al., PoS **LATTICE2023**, 181 (2024), arXiv:2311.03947 [hep-lat]]

Negative moment of inertia and magnetic gluon condensate

Taking the derivative at $\Omega = 0$, we obtain:

$$I = F_2 = T \frac{\partial^2 \log Z}{\partial \Omega^2}\bigg|_{\Omega=0} = T\big(\langle\!\langle S_1^2 \rangle\!\rangle_T + \langle\!\langle S_2 \rangle\!\rangle_T\big)\,,$$

where $\langle\!\langle \mathcal{O} \rangle\!\rangle_T = \langle \mathcal{O} \rangle_T - \langle \mathcal{O} \rangle_{T=0}$.
Using the exact forms of S_1, S_2, we get

$$I = I_{\text{mech}} + I_{\text{magn}}$$

where ($\langle J \rangle = 0$ for any T) and

$$I_{\text{mech}} = \frac{1}{T}\Big(\langle\!\langle J^2 \rangle\!\rangle_T - \langle\!\langle J \rangle\!\rangle_T^2\Big) \geq 0,$$

$$I_{\text{magn}} = \frac{1}{3}\int_V d^3x\, x_\perp^2 \langle\!\langle (F_{ij}^a)^2 \rangle\!\rangle_T = \frac{\alpha}{3} V R^2 \langle\!\langle (G_{\text{magn}})^2 \rangle\!\rangle_T\,.$$

J is the total angular momentum of gluon field.

- $I < 0$ for $T < T_s \simeq 1.5 T_c$ and $I > 0$ for $T > T_s$.
- Mass density $\rho_0(T) \leftrightarrow \langle\!\langle (G_{\text{magn}})^2 \rangle\!\rangle_T / 3$.

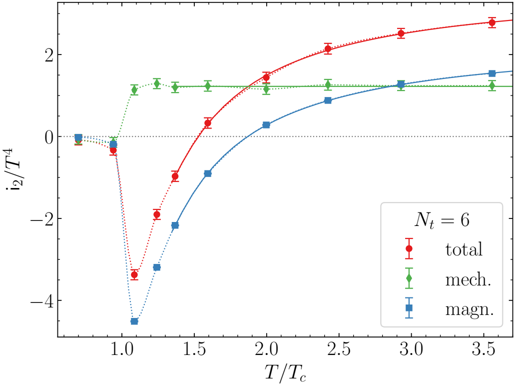

[V. V. Braguta et al., Phys. Rev. D **110**, 014511 (2024), arXiv:2310.16036 [hep-ph]]

Negative moment of inertia and magnetic gluon condensate

Taking the derivative at $\Omega = 0$, we obtain:

$$I = F_2 = T \frac{\partial^2 \log Z}{\partial \Omega^2}\bigg|_{\Omega=0} = T\left(\langle\!\langle S_1^2 \rangle\!\rangle_T + \langle\!\langle S_2 \rangle\!\rangle_T\right),$$

where $\langle\!\langle \mathcal{O} \rangle\!\rangle_T = \langle \mathcal{O} \rangle_T - \langle \mathcal{O} \rangle_{T=0}$.
Using the exact forms of S_1, S_2, we get

$$I = I_{\mathrm{mech}} + I_{\mathrm{magn}}$$

where ($\langle J \rangle = 0$ for any T) and

$$I_{\mathrm{mech}} = \frac{1}{T}\left(\langle\!\langle J^2 \rangle\!\rangle_T - \langle\!\langle J \rangle\!\rangle_T^2\right) \geq 0,$$

$$I_{\mathrm{magn}} = \frac{1}{3}\int_V d^3x\, x_\perp^2 \langle\!\langle (F_{ij}^a)^2 \rangle\!\rangle_T = \frac{\alpha}{3} V R^2 \langle\!\langle (G_{\mathrm{magn}})^2 \rangle\!\rangle_T .$$

J is the total angular momentum of gluon field.

- $I < 0$ for $T < T_s \simeq 1.5 T_c$ and $I > 0$ for $T > T_s$.
- Mass density $\rho_0(T) \leftrightarrow \langle\!\langle (G_{\mathrm{magn}})^2 \rangle\!\rangle_T / 3$.

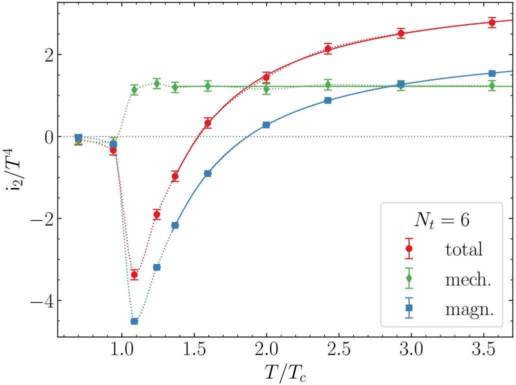

[V. V. Braguta et al., Phys. Rev. D **110**, 014511 (2024), arXiv:2310.16036 [hep-ph]]

Negative moment of inertia and magnetic gluon condensate

Taking the derivative at $\Omega = 0$, we obtain:

$$I = F_2 = T \frac{\partial^2 \log Z}{\partial \Omega^2}\bigg|_{\Omega=0} = T\Big(\langle\!\langle S_1^2 \rangle\!\rangle_T + \langle\!\langle S_2 \rangle\!\rangle_T\Big)\,,$$

where $\langle\!\langle \mathcal{O} \rangle\!\rangle_T = \langle \mathcal{O} \rangle_T - \langle \mathcal{O} \rangle_{T=0}$.
Using the exact forms of S_1, S_2, we get

$$I = I_{\mathrm{mech}} + I_{\mathrm{magn}}$$

where ($\langle J \rangle = 0$ for any T) and

$$I_{\mathrm{mech}} = \frac{1}{T}\Big(\langle\!\langle J^2 \rangle\!\rangle_T - \langle\!\langle J \rangle\!\rangle_T^2\Big) \geq 0,$$

$$I_{\mathrm{magn}} = \frac{1}{3}\int_V d^3x\, x_\perp^2 \langle\!\langle (F_{ij}^a)^2 \rangle\!\rangle_T = \frac{\alpha}{3} V R^2 \langle\!\langle (G_{\mathrm{magn}})^2 \rangle\!\rangle_T\,.$$

J is the total angular momentum of gluon field.

- $I < 0$ for $T < T_s \simeq 1.5 T_c$ and $I > 0$ for $T > T_s$.
- Mass density $\rho_0(T) \leftrightarrow \langle\!\langle (G_{\mathrm{magn}})^2 \rangle\!\rangle_T / 3$.

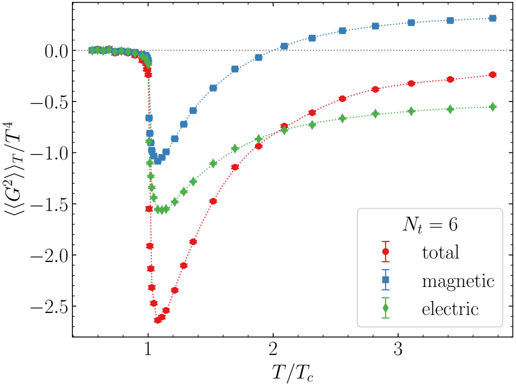

[V. V. Braguta et al., Phys. Rev. D **110**, 014511 (2024), arXiv:2310.16036 [hep-ph]]

- Gluon condensate evaporates at $T \gtrsim T_c$.
- $\langle\!\langle \mathcal{B}^2 \rangle\!\rangle$ reverse its sign at $\sim 2T_c$.

Negative moment of inertia and magnetic gluon condensate

Taking the derivative at $\Omega = 0$, we obtain:

$$I = F_2 = T \frac{\partial^2 \log Z}{\partial \Omega^2}\bigg|_{\Omega=0} = T\left(\langle\!\langle S_1^2 \rangle\!\rangle_T + \langle\!\langle S_2 \rangle\!\rangle_T\right),$$

where $\langle\!\langle \mathcal{O} \rangle\!\rangle_T = \langle \mathcal{O} \rangle_T - \langle \mathcal{O} \rangle_{T=0}$.
Using the exact forms of S_1, S_2, we get

$$I = I_{\text{mech}} + I_{\text{magn}}$$

where ($\langle J \rangle = 0$ for any T) and

$$I_{\text{mech}} = \frac{1}{T}\left(\langle\!\langle J^2 \rangle\!\rangle_T - \langle\!\langle J \rangle\!\rangle_T^2\right) \geq 0,$$

$$I_{\text{magn}} = \frac{1}{3}\int_V d^3x\, x_\perp^2 \langle\!\langle (F_{ij}^a)^2 \rangle\!\rangle_T = \frac{\alpha}{3} V R^2 \langle\!\langle (G_{\text{magn}})^2 \rangle\!\rangle_T .$$

J is the total angular momentum of gluon field.

- $I < 0$ for $T < T_s \simeq 1.5 T_c$ and $I > 0$ for $T > T_s$.
- Mass density $\rho_0(T) \leftrightarrow \langle\!\langle (G_{\text{magn}})^2 \rangle\!\rangle_T / 3$.

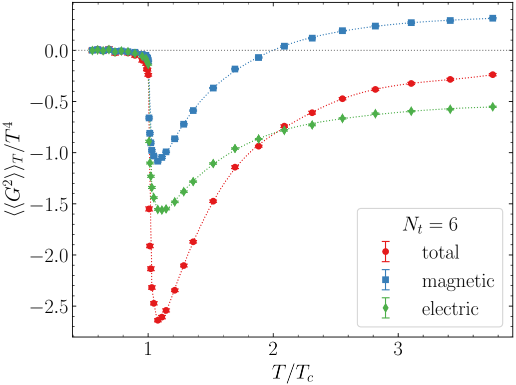

[V. V. Braguta et al., Phys. Rev. D **110**, 014511 (2024), arXiv:2310.16036 [hep-ph]]

- Gluon condensate evaporates at $T \gtrsim T_c$.
- $\langle\!\langle \mathcal{B}^2 \rangle\!\rangle$ reverse its sign at $\sim 2T_c$.
- In QCD fermionis contribute only to I_{mech}.

Total angular momentum $\boldsymbol{J} = I\boldsymbol{\Omega}$ is a sum of the orbital and spin parts:

$$\boldsymbol{J} = \boldsymbol{L} + \boldsymbol{S}\,, \tag{24}$$

and $I < 0$. The possible physical picture: ▷ instability, or ▷ *negative* Barnett effect for gluon.

Total angular momentum $\boldsymbol{J} = I\boldsymbol{\Omega}$ is a sum of the orbital and spin parts:

$$\boldsymbol{J} = \boldsymbol{L} + \boldsymbol{S}\,, \tag{24}$$

and $I < 0$. The possible physical picture: ▷ instability, or ▷ *negative* Barnett effect for gluon.

In the temperature range $T_c \lesssim T < T_s \simeq 1.5T_c$:

(i) a sizable fraction of the total angular momentum $\boldsymbol{J} = \boldsymbol{L} + \boldsymbol{S}$ is accumulated in the spin of gluons $\boldsymbol{S}$;

(ii) therefore, $\boldsymbol{S} \uparrow\uparrow \boldsymbol{J}$ and $\boldsymbol{S} \uparrow\downarrow \boldsymbol{L}$.

Let's introduce $\boldsymbol{L} = I_L\boldsymbol{\Omega}$, $\boldsymbol{S} = I_S\boldsymbol{\Omega}$, therefore

$$I_L > 0\,, \quad I_S < 0\,, \quad I = I_L + I_S < 0\,.$$

(negative spin-vortical coupling for gluons)

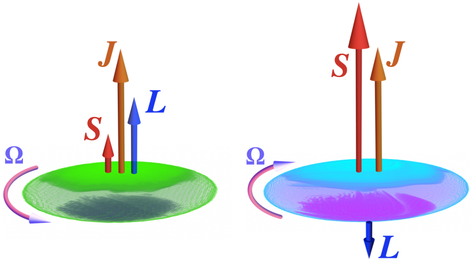

(left) usual Barnett effect
(right) negative Barnett effect
[V. V. Braguta et al., Phys. Rev. D **110**, 014511 (2024), arXiv:2310.16036 [hep-ph]]

Inhomogeneous phase in QCD (preliminary)

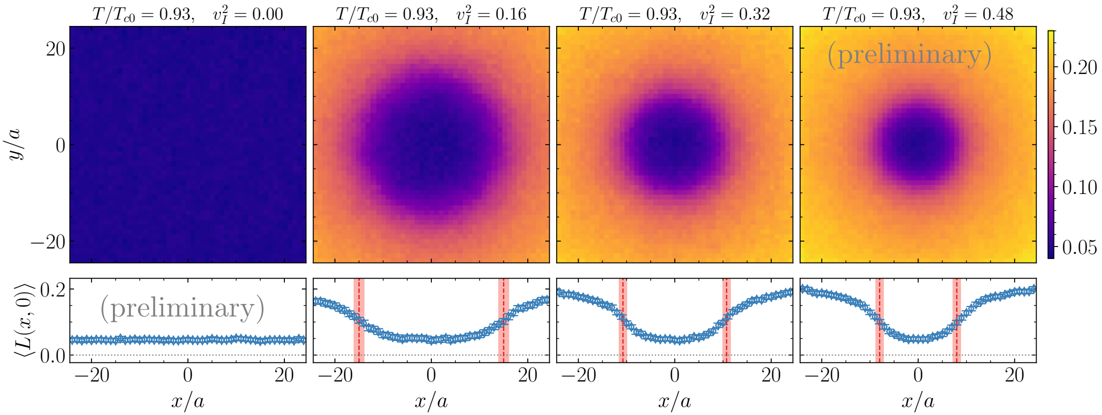

Figure: The distribution of the local Polyakov loop in x, y-plane for the lattice of size $4 \times 20 \times 49^2$ at the fixed temperature $T = 0.93\,T_{c0}$ and different v_I; QCD with Wilson fermions (Iwasaki action), $m_\pi / m_\rho = 0.80$.

- Mixed inhomogeneous phase takes place also in QCD! (work in progress . . .)
- On the rotation axis, the spin-rotating coupling term only survives.

Rigid rotation vs spin potential

Angular velocity, Ω

$$\delta_\Omega \mathcal{L}_q = \Omega\,\bar\psi\big[i(-x\partial_y + y\partial_x) + \gamma^0\Sigma^{12}\big]\psi\,,$$
$$\delta_\Omega \mathcal{L}_G = \frac{1}{2g^2}\Big[2r\Omega\left(F^a_{\hat\varphi r}F^a_{rt} + F^a_{\hat\varphi z}F^a_{zt}\right) - r^2\Omega^2\left(F^a_{\hat\varphi z}F^a_{\hat\varphi z} + F^a_{r\hat\varphi}F^a_{r\hat\varphi}\right)\Big],$$

▷ At the rotation axis, $x = y = 0$, the local action of rotating system coincides with the system at finite spin density of quarks, $\Omega = \mu_\Sigma$.

Spin potential, μ_Σ

$$\delta_\Sigma \mathcal{L}_q = \mu_\Sigma\,\bar\psi\gamma^0\Sigma^{12}\psi = \frac{1}{2}\mu_\Sigma\,\bar\psi\gamma^3\gamma^5\psi$$

(simulation with imaginary μ_Σ^{I}; similar to quark chemical potential)

▷ The system at finite μ_Σ is homogeneous, unlike the case of rotating system.

▷ In the approximation of "local thermalization", the results for finite μ_Σ describes the shift of local T_c at the axis, $r = 0$, for mixed phase in rotating QCD.

Lattice action and setup

In continuum notations, the Euclidean quark action at the finite spin potential μ_Σ has the following form:

$$S_F = \int d^4x\, \bar{\psi}\Big[\gamma^x D_x + \gamma^y D_y + \gamma^z D_z + \gamma^\tau \big(D_\tau + i\mu_\Sigma^{\mathrm{I}} \Sigma^{12}\big) + m\Big]\psi\,. \tag{25}$$

- We use $N_f = 2$ clover-improved Wilson fermions (c_{SW} from one-loop) + RG-improved (Iwasaki) gauge action.
- The spin density term is exponentiated like quark chemical potential.
- Simulations are performed on lattices of the size 4×16^3, 5×20^3, 6×24^3 for meson mass ratios $m_{\mathrm{PS}}/m_{\mathrm{V}} = 0.60, \ldots, 0.85$.
- Due to competition between quarks and gluons in rotating system, the dependence of the results on the pion mass is of a particular interest.
- Temperature is $T = 1/(N_t a)$.

- V. V. Braguta, M. N. Chernodub, and A. A. Roenko, Phys. Rev. D **111**, 114508 (2025), arXiv:2503.18636 [hep-lat]

Observables

Deconfinement crossover

In QCD, the Polyakov loop is an approximate order parameter (exact for gluodynamics, $m_q \to \infty$),

$$L = \frac{1}{N_s^3} \sum_{\vec{r}} \mathrm{Tr}\left[\prod_{\tau=0}^{N_t-1} U_4(\vec{r},\tau)\right], \tag{26}$$

In confinement $\langle L \rangle \approx 0$; in deconfinement $\langle L \rangle \neq 0$. $\langle L \rangle = e^{-F_Q/T}$
The deconfinement crossover temperature is associated with the peak of the Polyakov loop susceptibility

$$\chi_L = \langle |L|^2 \rangle - \langle |L| \rangle^2 . \tag{27}$$

Chiral crossover

The chiral condensate, $\langle \bar{\psi}\psi \rangle$, is an exact order parameter for massless case ($m_q \to 0$).
The chiral crossover temperature is determined using the (disconnected) chiral susceptibility:

$$\chi_{\bar{\psi}\psi}^{\mathrm{disc}} = \frac{N_f T}{V}\left[\left\langle \mathrm{Tr}(M^{-1})^2 \right\rangle - \left\langle \mathrm{Tr}(M^{-1}) \right\rangle^2\right]. \tag{28}$$

At low temperatures chiral symmetry is broken, $\langle \bar{\psi}\psi \rangle \neq 0$, and it is restored at high temperatures $\langle \bar{\psi}\psi \rangle = 0$.

Polyakov loop susceptibility and chiral susceptibility

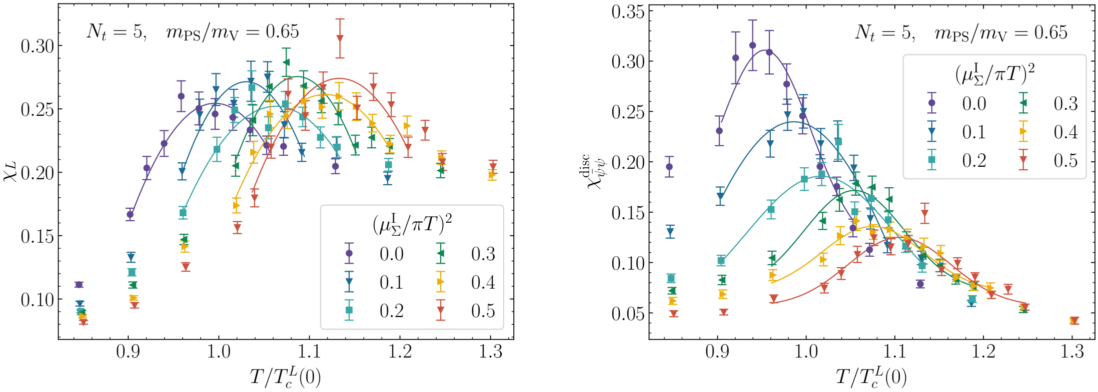

Figure: The susceptibilities of the Polyakov loop and the chiral condensate as a function of temperature.

- Pseudo-critical temperatures increases with an imaginary spin potential.
- The finite (imaginary) spin density softens the chiral phase transition $\Rightarrow$ The real spin density makes the transition sharper, and CEP is expected for chiral transition (but not for deconfinement).

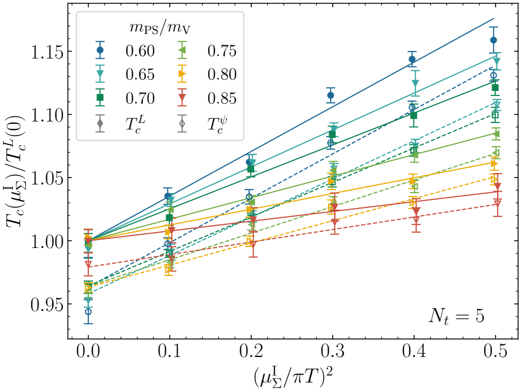

We fit the data by the quadratic function of the imaginary spin potential $\mu_\Sigma^{\rm I}$:

$$T_c^\ell(\mu_\Sigma^{\rm I}) = T_c^\ell(0)\left[1 + \kappa_\Sigma^\ell\left(\frac{\mu_\Sigma^{\rm I}}{T}\right)^2\right], \qquad (29)$$

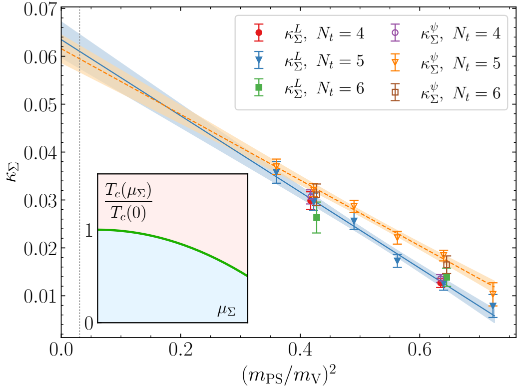

We fit the data by the quadratic function of the imaginary spin potential $\mu^{\rm I}_\Sigma$:

$$T^\ell_c(\mu^{\rm I}_\Sigma) = T^\ell_c(0)\left[1 + \kappa^\ell_\Sigma\left(\frac{\mu^{\rm I}_\Sigma}{T}\right)^2\right], \qquad (29)$$

$$T^\ell_c(\mu_\Sigma) = T^\ell_c(0)\left[1 - \kappa^\ell_\Sigma\left(\frac{\mu_\Sigma}{T}\right)^2\right]. \qquad (30)$$

The dependence of the coefficients κ^ℓ_Σ $(\ell = L, \psi)$ on the pion mass ratio can be well described by

$$\kappa^\ell_\Sigma(\xi) = k^\ell_\Sigma + \gamma^\ell_\Sigma\,\xi^2\,, \qquad \xi = \frac{m_{\rm PS}}{m_{\rm V}}. \qquad (31)$$

In the limit of physical pion mass,

$$\kappa^{L\ (\rm phys)}_\Sigma = 0.0610(35)\,, \qquad \kappa^{\psi\ (\rm phys)}_\Sigma = 0.0595(27)\,, \qquad \text{at} \quad \left(\frac{m_{\rm PS}}{m_{\rm V}}\right)_{\rm phys} = 0.175\ .$$

For $\mu_\Sigma \sim 10$ MeV, $\Delta T/T \sim 0.03$ %.

For baryon density, the coefficient is $\kappa_q \sim 0.12(2)$.

Conclusions

- We found the mixed phase in rotating gluodynamics at thermal equilibrium. The same is expected for QCD (in progress).
- For *imaginary* rotation, it takes place for $T < T_{c0}$ with deconfinement (confinement) phase at the periphery (center).
- For *real* rotation, the inhomogeneous phase may arise for $T > T_{c0}$ with confinement at the periphery and deconfinement in the center.
- We demonstrate the validity of analytic continuation using Im2/Re2-regimes.

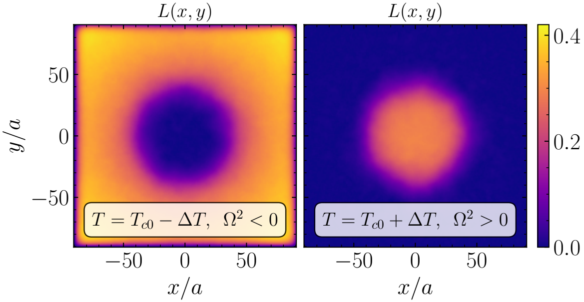

- The local critical temperature in rotating gluodynamics increases with the (real) local velocity $u = \Omega r$. The approximation of local thermalization gives consistent results. Note that $T_c(0) \approx T_{c0}$.
- The magnetovortical coupling generates asymmetry in the action for chromomagnetic fields. Linear coupling (source of SP) play subleading role near T_c. This mechanism can not be accounted for by TE.
- Gluon plasma has $I < 0$ below the supervortical temperature $T_s = 1.50(10) T_c$ (and $I > 0$ for $T > T_s$). Possible physical explanation: NBE. Results for a.c. from Ω_I and $\partial_\Omega|_{\Omega=0}$ are in agreement.
- QCD at non-zero spin density describe the effects on the rotational axis of large system. For the spin potential $\mu_\Sigma = 10\,\mathrm{MeV}$, the crossover temperatures T^L and T^ψ drop only by about 0.03%.

Thank you for your attention!

Imaginary vs real rotation for different regimes

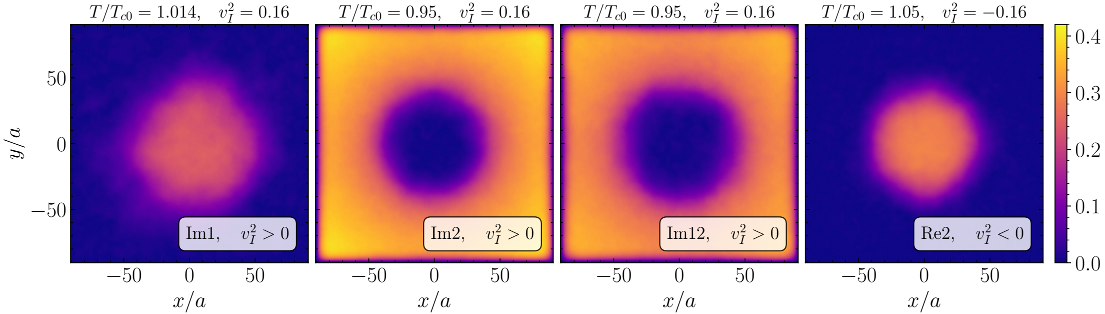

Figure: The distribution of the local Polyakov loop in x, y-plane for lattice size $5 \times 30 \times 181^2$, open boundary conditions (OBC) at fixed velocity $|v_I^2| = 0.16$ and different regimes. Temperature was chosen to see mixed phase.

- In the regimes Im1 and Re2, the rotation produces confinement phase in the outer region at $T > T_{c0}$. Regime Re2 realizes real rotation for S_2 system.
- Phase arrangement is the same in Im2- and Im12-regimes. The radius of the inner region in regime Im2 is slightly smaller, than in regime Im12.

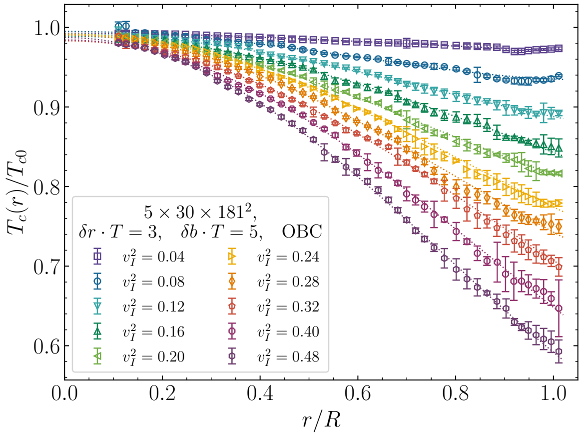

- The results in the whole region are well described by the quartic formula

$$\frac{T_c(r)}{T_{c0}} = C_0 - C_2 \left(\frac{r}{R}\right)^2 + C_4 \left(\frac{r}{R}\right)^4 . \quad (32)$$

- In the bulk, $r/R \lesssim 0.5$, quadratic fit is sufficient $(C_4 = 0)$.

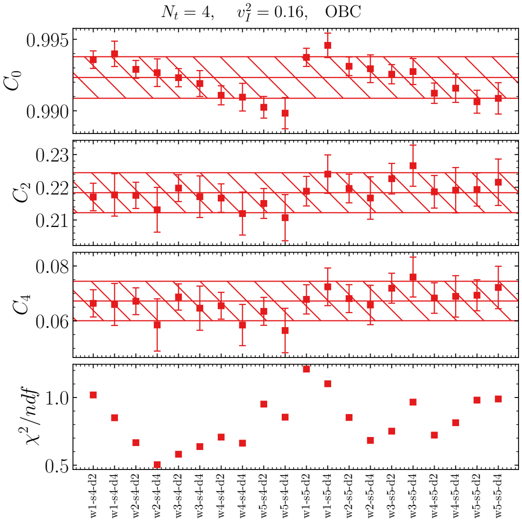

- The results in the whole region are well described by the quartic formula

$$\frac{T_c(r)}{T_{c0}} = C_0 - C_2\left(\frac{r}{R}\right)^2 + C_4\left(\frac{r}{R}\right)^4 . \quad (32)$$

- In the bulk, $r/R \lesssim 0.5$, quadratic fit is sufficient ($C_4 = 0$).

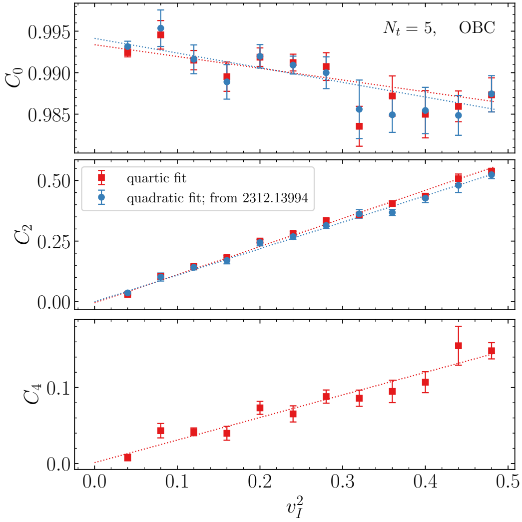

- The results in the whole region are well described by the quartic formula

$$\frac{T_c(r)}{T_{c0}} = C_0 - C_2\left(\frac{r}{R}\right)^2 + C_4\left(\frac{r}{R}\right)^4 . \quad (32)$$

- In the bulk, $r/R \lesssim 0.5$, quadratic fit is sufficient ($C_4 = 0$).

- We found numerically that

$$C_i(v_I^2) = a_i + \kappa_i v_I^2 . \quad (33)$$

- $T_c(0) \approx T_{c0}$ with few percent accuracy:
  - Effects of finite radius R.
  - Effects of averaging in layers of width δr.

Local critical temperature

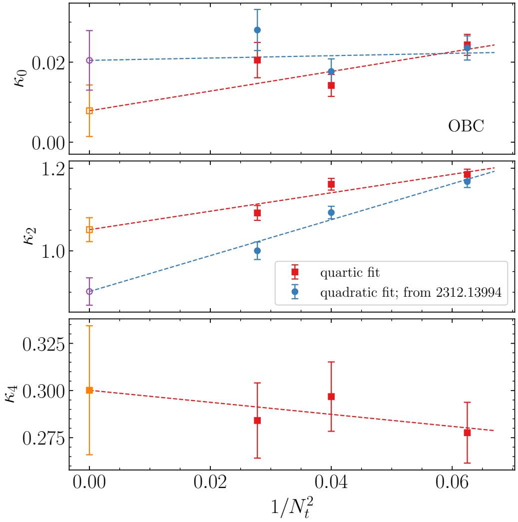

- Results: The local critical temperature decreases with imaginary angular velocity.

$$\frac{T_c(r,\Omega_I)}{T_{c0}} = 1 - (\Omega_I r)^2 \left(\kappa_2 - \kappa_4 \left(\frac{r}{R}\right)^2\right). \quad (34)$$

- The vortical curvature in continuum limit from quadratic fit ($r/R \lesssim 0.5$) is universal

$$\kappa_2 = 0.902(33)\,, \quad (35)$$

- And from quartic fit (for OBC) there is

$$\kappa_2 = 1.051(29)\,, \qquad \kappa_4 = 0.300(34)\,, \quad (36)$$

where κ_4 term is a finite volume correction;

- We can not distinguish $\sim \Omega^4$ term.

Finite radius effects

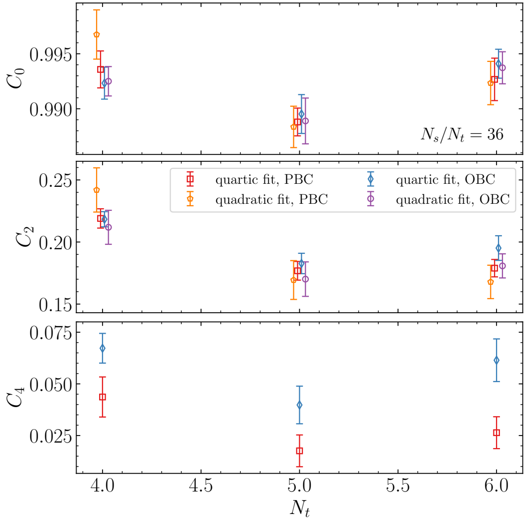

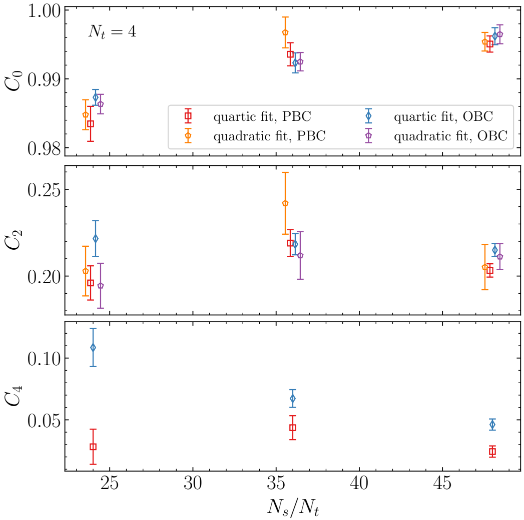

Local Polyakov loop at high temperatures

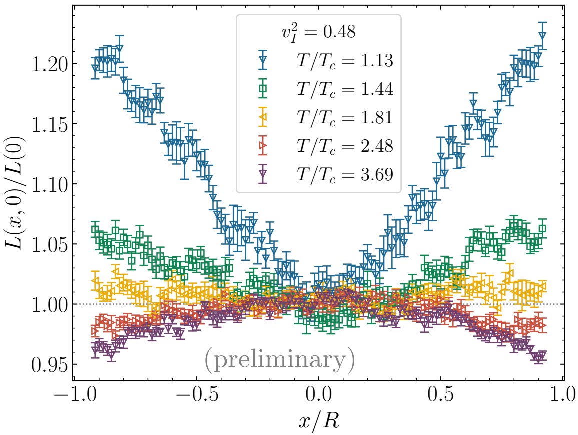

- $T > T_s \simeq 1.5 T_{c0}$: $\quad I > 0$
- $T \gtrsim 2T_{c0}$: $\quad \langle\langle \mathcal{B}^2 \rangle\rangle > 0$
- Local Polyakov loop decreases with r at high temperatures $T \gtrsim 2T_{c0}$

  (local temperature from TE decreases with r for imaginary Ω_I)

Pseudo-critical temperatures: lattice spacing effects

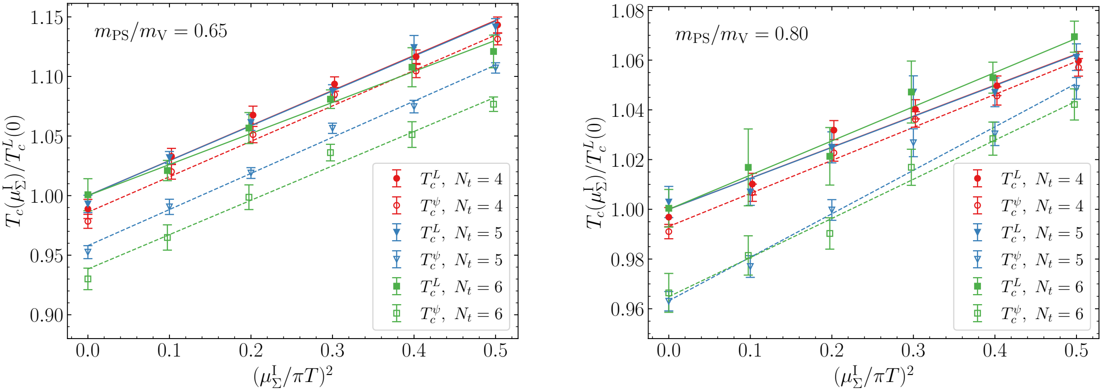

Figure: Transition temperatures T_c of the deconfinement and chiral crossovers as a function of spin potential.

- Pseudo-critical temperatures increases with an imaginary spin potential.
- There is a weak dependence of the results on the lattice spacing a.

Rotating QCD: various rotation regimes

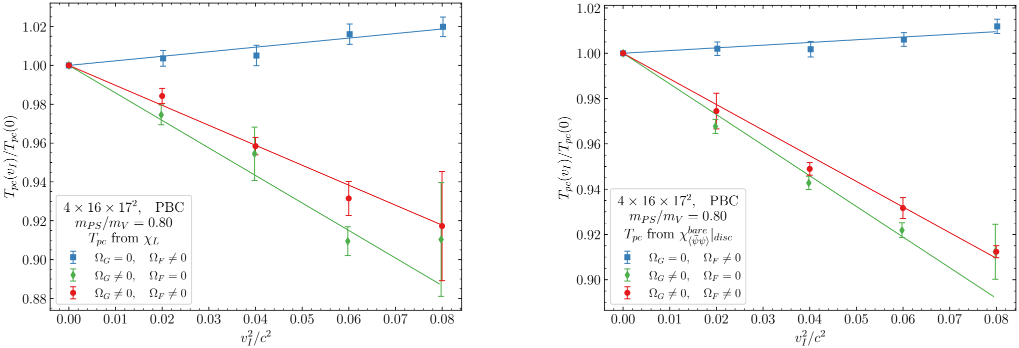

Figure: The (bulk-averaged) pseudo-critical temperature as a function of imaginary linear velocity on the boundary for various rotation regimes (full, only gluons, only fermions). [V. Braguta et al., PoS **LATTICE2022**, 190 (2023), arXiv:2212.03224 [hep-lat]]

QCD action: $S = S_G(\Omega_G) + S_F(\Omega_F)$

Rotation in fermionic sectors has similar to S_1 influence on (bulk-averaged) T_{pc}. Gluons (S_2) dominate.